Structural features of the La-Sr-Fe-Co-O system

Á. Cziráki[1], I. Gerőcs[1], M. Köteles[1], A. Gábris[1], L. Pogány[2], I. Bakonyi[2,a], Z. Klencsár[3], A. Vértes[3], S.K. De[4],
A. Barman[4], M. Ghosh[4], S. Biswas[4], S. Chatterjee[4], B. Arnold[5], H.D. Bauer[5], K. Wetzig[5],
C. Ulhaq-Bouillet[6], and V. Pierron-Bohnes[6]

[1] Department of Solid State Physics, Eötvös University, 1518 Budapest, POB 32, Hungary
[2] Research Institute for Solid State Physics and Optics, Hungarian Academy of Sciences, 1525 Budapest, POB 49, Hungary
[3] Research Group for Nuclear Methods in Structural Chemistry of the Hungarian Academy of Sciences,
    Department of Nuclear Chemistry, Eötvös University, 1518 Budapest, POB 32, Hungary
[4] Department of Materials Science, Indian Association for the Cultivation of Science, Jadavpur, Calcutta 700032, India
[5] Institut für Festkörper- und Werkstofforschung, Helmholtzstrasse 20, 01069 Dresden, Germany
[6] Institut de Physique et Chimie des Matériaux de Strasbourg, UMR C75040 CNRS-ULP, 23 rue du Loess,
    67037 Strasbourg, France

Abstract. A structural study has been performed on the $La_{0.8}Sr_{0.2}Fe_xCo_{1-x}O_3$ ($x = 0.025$ to 0.3) system displaying large magnetoresistance (MR) at room temperature. A detailed analysis of the crystal structure and microstructure was done by X-ray diffraction (XRD), transmission and scanning electron microscopy (TEM and SEM). The atomic resolution TEM images and the appearing superreflections in the corresponding SAED patterns revealed that a superstructure is formed due to the presence of iron. The correlation between the ordered microstructure and the observed large MR ratio is discussed. ^{57}Fe Mössbauer spectroscopy was utilized to gain information on the valence state of iron in the sample with $x = 0.3$. The lattice parameters of Fe- doped $La_{0.8}Sr_{0.2}Fe_xCo_{1-x}O_3$ compounds were found to increase monotonously with increasing Fe content. The valence state of iron was found to be Fe^{3+}.

PACS. 75.30.Vn Colossal magnetoresistance – 61.72.-y Defects and impurities in crystals; microstructure – 72.15.Gd Galvanomagnetic and other magnetotransport effects

1 Introduction

The $La_{0.8}Sr_{0.2}Fe_xCo_{1-x}O_3$ system with x ranging from 0.025 up to 0.3 exhibits a large magnetoresistance (MR) ratio at room temperature, thus promising important technological applications [1]. The parent compound of this system, $LaCoO_3$, is a non-magnetic insulator below $T = 50$ K. At higher temperatures, it displays anomalous electrical and magnetic properties which are governed mainly by the $3d$ orbitals of Co. In $LaCoO_3$, the crystal field splitting between the t_{2g} and e_g states of Co^{3+} is comparable to the Hund coupling energy that causes a temperature dependent spin state transition between the low-spin state $t_{2g}^6 e_g^0$ ($S = 0$) and high-spin state $t_{2g}^4 e_g^2$ ($S = 2$) of Co^{3+} ions. Such a transition from the low-spin state to the high-spin state is accompanied by a semiconductor-to-metal phase transition around 500 K [2].

The Sr^{2+}-doped lanthanum cobaltite, $La_{1-y}^{3+}Sr_y^{2+}CoO_{3-\delta}$, behaves like a doped semiconductor for $y < 0.18$, and exhibits an insulator-to-metal transition in the range $y = 0.18$ to 0.2 [3–7]. Large magnetoresistance has been observed in the $La_{1-y}Sr_yCoO_3$ system with $y \leq 0.15$ at temperatures below $T = 100$ K [7–9]. At the

same time, the magnetoresistance for the $La_{1-y}Sr_yCoO_3$ system with $y \leq 0.25$ was found to be close to zero at room temperature [7].

The substitution of Fe for Co in the $La_{1-y}Sr_yCoO_3$ system has been found to have a strong effect on the magnetic and electrical properties, including magnetoresistance [1]. Upon the substitution of Fe for Co, the compounds $La_{0.8}Sr_{0.2}Fe_{1-x}Co_xO_3$ ($x = 0.025$ to 0.3) become semiconductor, and up to $T = 300$ K, a semiconductor-to-metal transition was not observed. At the same time, as an effect of the iron substitution, very large MR was observed below $T = 50$ K and from $T = 150$ K up to at least room temperature [1].

The aim of the present work was to perform a detailed study of the structural changes caused by iron doping in order to gain a deeper insight into the role of the structural evolution in the realization of the unusual magnetoresistance above $T = 150$ K.

2 Experimental

Polycrystalline samples with the nominal composition of $La_{0.8}Sr_{0.2}Fe_xCo_{1-x}O_3$ ($x = 0.025, 0.05, 0.10, 0.15, 0.20, 0.3$) were prepared *via* solid state reactions. Stoichiometric

a e-mail: bakonyi@szfki.hu

Table 1. EDX analysis results on the $La_{0.8}Sr_{0.2}Fe_xCo_{1-x}O_3$ samples. The Fe-content and the Sr-content were determined from the measured Co/Fe and La/Sr concentration ratios, respectively.

nominal Fe-content	0.025	0.05	0.10	0.20	0.30
measured Fe-content	0.026	0.05	0.10	0.21	0.32
measured Sr-content	0.25	0.26	0.30	0.30	0.25

amounts of La_2O_3, $SrCo_3$, Co_3O_4, Fe_2O_3 mixed with distilled ethanol were dried and calcined in open air at 800 °C for 24 h. The calcined powders were then ground, pressed into pellets, and sintered in open air first at 1000 °C, and afterwards at 1200 °C for 24 h.

A detailed analysis of the crystal structure was performed by X-ray diffraction (XRD) measurements using a Philips X'Pert equipment. The 2θ angle was step-scanned from 10° to 90° with a step width of 0.02° and an integration time of 2 s. The crystal structure of the samples was refined using a powder X-ray FullProf program [10].

The crystal structure and the microstructure of the samples was studied conventional and atomic-resolution transmission electron microscopy (TEM). The chemical composition was measured by energy-dispersive X-ray (EDX) analysis in a scanning electron microscope.

A ^{57}Fe Mössbauer study was performed at room temperature on the sample with the composition $La_{0.8}Sr_{0.2}Co_{0.7}Fe_{0.3}O_3$. The measurement was done on a powdered sample in transmission geometry. A ^{57}Co(Rh) source with 25 mCi activity provided the γ-rays. The Mössbauer spectrum was analyzed by the MossWinn program [11].

3 Results

The actual average composition of the samples as determined by EDX analysis is shown in Table 1. While the measured Fe concentration corresponds well to the nominal one in each of the investigated samples, the measured Sr content turns out to be higher than the nominal value. By considering that around the Sr content $y = 0.2$ to 0.25, the iron-free system displays abrupt changes in its crystal structure as well as in its conductivity behavior [3], this finding may prove to be important in the interpretation of the anomalous high MR ratio (Fig. 1) observed for the iron-containing compound at room temperature [1].

The large MR ratio observed for the compounds $La_{0.8}Sr_{0.2}Fe_xCo_{1-x}O_3$, even with an iron content as low as $x = 0.025$, indicates that iron plays a key role in the realization of the high MR ratio observed above $T = 150$ K [1]. This effect of iron can be connected to a change in the microstructure of the iron-doped materials.

The crystal structure of the $LaCoO_3$ system is known as a rhombohedral one with R-3m space group. As an effect of Sr doping, the space group of the crystal structure changes to R-3c in $La_{1-y}Sr_yCoO_3$ for Sr-contents $y < 0.5$ [3]. Accordingly, as a first trial, we made an attempt to analyze the powder XRD patterns of the iron-doped
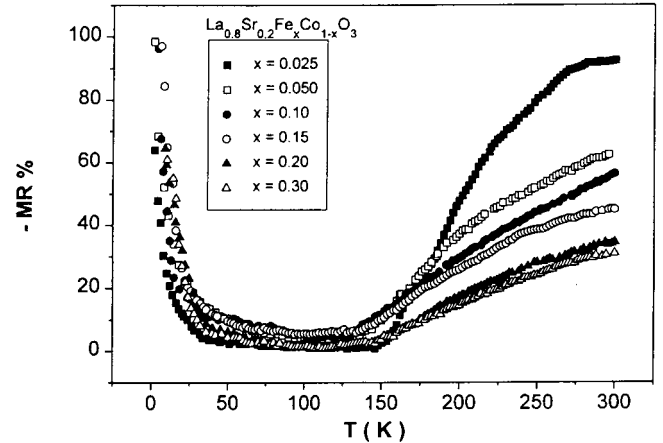

Fig. 1. Magnetoresistance (MR) ratio *versus* temperature for $La_{0.8}Sr_{0.2}Fe_xCo_{1-x}O_3$ ($x = 0.025-0.3$) compounds at a magnetic field of 7.5 T [1]. The magnetoresistance was defined as $MR = [R(H) - R(0)]/R(0)$ where $R(H)$ and $R(0)$ refer to the resistance in a magnetic field H and in zero magnetic field, respectively.

samples by assuming the same rhombohedral R-3c crystal structure. The open symbols in Figure 2 show the lattice parameter values obtained in this way as a function of the Fe-content.

Despite the reasonable agreement between the measured and the calculated rhombohedral R-3c XRD profiles (the "goodness of fit" was $\chi^2 \approx 5$), the TEM selected-area electron diffraction (SAED) patterns revealed a contradiction. Namely, the SAED patterns could not be indexed appropriately on the basis of this rhombohedral crystal structure. According to the suggestion of the results of the SAED patterns, the XRD profiles were refitted by using the original R-3m space group of the $LaCoO_3$ structure, but in this case the half value of the c-axis was used in the hexagonal representation. This cell in the rhombohedral representation corresponds to a slightly deformed cubic perovskite type structure. The filled symbols in Figure 2 show the lattice parameters obtained from the fitting of the measured XRD profiles using this R-3m space group. This structure fits practically equally well the experimental profiles as the R-3c one and the obtained lattice parameters increase similarly with increasing Fe content for both space group structures (Fig. 2).

The open triangle and circle in Figure 2 show the lattice parameters for the iron-free compound for two Sr-contents as indicated from reference [3], in order to see the influence of the nominal and measured Sr-contents in our samples. On the basis of Figure 2 and Table 1 it can be established that the observed lattice parameter change can indeed be ascribed to the Fe-doping.

On the basis of the width of the measured XRD peaks, the average grain size has been estimated using the Williamson and Hall method. In the investigated samples, the average grain size was found to be between 50 nm and 80 nm. At the same time, TEM pictures (Fig. 3) indicated a grain size of about 1 μm. The atomic resolution TEM investigations revealed that the apparently large grains
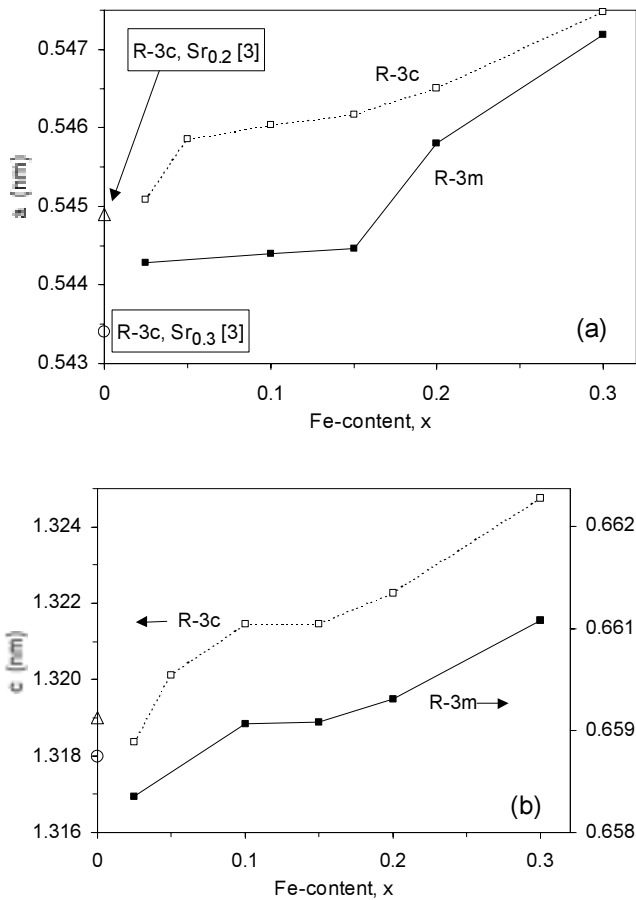
Fig. 2. Lattice parameter values derived from the XRD patterns of the $La_{0.8}Sr_{0.2}Fe_xCo_{1-x}O_3$ samples. The open symbols refer to a fitting to a rhombohedral crystal structure with the R-3c space group and the filled symbols to a slightly deformed cubic perovskite type crystal structure with the R-3m space group. The open triangle and circle refer to the iron-free compound lattice parameters for the Sr-contents as indicated from reference [3].

consist of randomly arranged very fine (at some places as small as 5 nm) crystallites (Fig. 4). Some places of the samples exhibit a very characteristic ordered domain structure (Fig. 5). The volume fraction of these ordered domains increases with increasing Fe content.

The SAED study revealed differently ordered structures between the small domains. Figure 6 shows typical SAED patterns taken from the ⟨001⟩ direction. In spite of the fact that these SAED patterns contain diffraction spots given by more than one crystallite, it is possible to select the spots arising from a selected crystallite, namely that oriented exactly in the (001) direction, by neglecting spots due to the neighbouring crystallites which give reflection spots in some cases very close to the strongest spots of the selected crystallite. The sketches attached to the SAED patterns of Figure 6 visualize which spots arise from the selected individual crystallite only. The weak su-
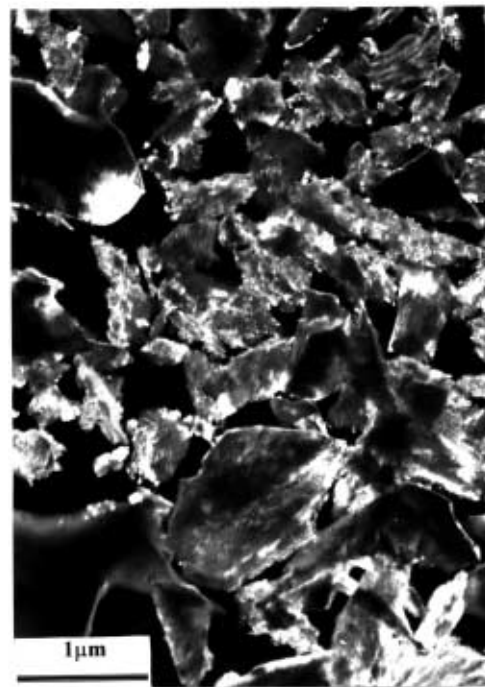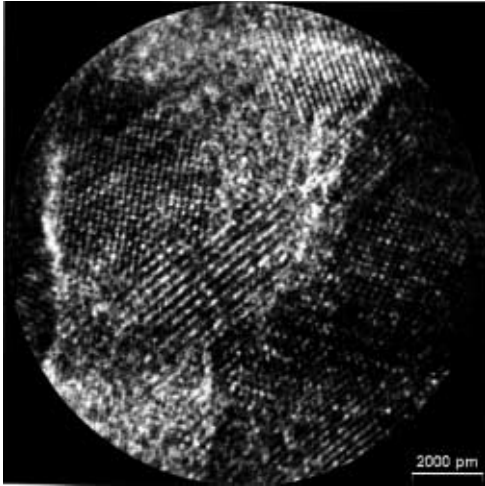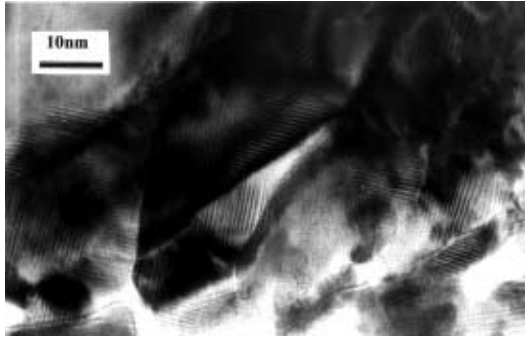

Fig. 3. Conventional TEM pictures taken in (a) bright-field and (b) dark-field mode on the $La_{0.8}Sr_{0.2}Fe_{0.025}Co_{0.975}O_3$ sample.

perreflections denoted by crosses (×) indicate that either lattice doubling (Fig. 6a) or tripling (Fig. 6b) takes place in the given areas.

Fig. 4. Atomic resolution TEM picture taken on the $La_{0.8}Sr_{0.2}Fe_{0.20}Co_{0.80}O_3$ sample.

Fig. 5. TEM picture of the characteristic domain structure detected in the $La_{0.8}Sr_{0.2}Fe_{0.05}Co_{0.95}O_3$ sample.

The same phenomena appear in the SAED patterns shown in Figure 7. These diffraction pictures are taken from the $\langle 021 \rangle$ direction, and they exhibit weaker extra spots at the half-length of the (224) type reflections in the case of the samples with low Fe content (Fig. 7a). At higher Fe concentrations, the weak spots appear at the half (Fig. 7b) and at the quarter (Fig. 7c) of the (200) reflection that confirms the lattice doubling in this direction. This finding indicates that an ordered substitution of the Co atoms by Fe atoms takes place in the investigated $La_{0.8}Sr_{0.2}Fe_xCo_{1-x}O_3$ compounds. The encountered superreflections provide a direct evidence for the ordering phenomena being a consequence of the ordered lattice substitution between La/Sr or Co/Fe atoms.

The existence of locally ordered domain structures which are caused by composition fluctuations is also evident from the high-resolution TEM picture taken on the compound $La_{0.8}Sr_{0.2}Fe_{0.3}Co_{0.7}O_3$ (Fig. 8). An anisotropic ordered perovskite-type structure originating from the ordered lattice substitution clearly visualizes itself in the Fourier pattern of this picture as extra spots of the superstructure.

Figure 9 shows the room temperature ^{57}Fe Mössbauer spectrum of $La_{0.8}Sr_{0.2}Fe_{0.3}Co_{0.7}O_3$. The spectrum displays a quadrupole doublet with a quadrupole splitting of $QS = 0.389(4)$ mm/s and isomer shift of $IS = 0.322(2)$ mm/s relative to α-Fe at room temperature. The individual lines of the doublet are rather broad, and they can not be fitted appropriately with the usual Lorentzian line shape. Therefore, two identical Voigt absorption line profiles were used to fit the spectrum, which resulted in a very good fit, the normalized χ^2 value being 0.812. The width of the Gaussian and Lorentzian lines building up the Voigt absorption line turned out to be $\Gamma_G = 0.31(2)$ mm/s and $\Gamma_L = 0.29(2)$ mm/s, respectively.

4 Discussion

As an effect of the partial substitution of La^{3+} with Sr^{2+} cations in $La_{0.8}Sr_{0.2}Fe_xCo_{1-x}O_3$, the excess charge induced by Sr-doping can be compensated either by the oxidation of a corresponding amount of Co^{3+} to Co^{4+}, or by the creation of oxygen vacancies. These alternative processes compete with each other. An earlier study of the oxygen non-stoichiometry of the $La_{1-y}Sr_yCoO_3$ system [12] revealed that the oxidation of Co^{3+} to Co^{4+} is preferable for $y < 0.5$. A similar tendency was reported in reference [3], where the creation of oxygen vacancies was recognized already for $y < 0.5$. Namely, an increasing deviation from the nominal oxygen stoichiometry, indicating the creation of oxygen vacancies, was observed for $y \geq 0.2$. Additionally, the lattice parameters were found to display an anomalous behavior in the range of $0.2 < y < 0.4$ [3]. The detected abrupt changes in the lattice parameters were attributed to the appearance of oxygen vacancies.

According to the results of the present XRD measurements, the lattice parameters of the $La_{0.8}Sr_{0.2}Fe_xCo_{1-x}O_3$ system increase monotonously with increasing Fe-content (Fig. 2). Taking into account the fact that the Fe^{3+}, Co^{3+} and Co^{4+} ions have almost identical radii [13], the detected lattice parameter increase may be an indication that in the presence of iron the creation of oxygen vacancies, induced by Sr-doping, is more favorable. Namely, the increasing amount of oxygen vacancies is expected to result in an expansion of the perovskite-type lattice.

Fe^{3+} having an electronic structure similar to that of Co^{4+} is expected to replace Co^{4+}, thus promoting the creation of oxygen vacancies against the oxidation of the Co^{3+} ions. This mechanism is also supported by the ^{57}Fe Mössbauer spectrum of $La_{0.8}Sr_{0.2}Fe_{0.3}Co_{0.7}O_3$. Namely, the observed ^{57}Fe Mössbauer isomer shift is clearly indicative for Fe^{3+}. Furthermore, in this system the observation of a non-zero quadrupole splitting can be attributed to the existence of an oxygen vacancy in the neighborhood of Fe^{3+} [14]. Moreover, the obtained IS and QS Mössbauer parameters are almost the same as those observed earlier for Fe^{3+} in oxygen deficient $Sr_3Fe_2O_{6.2}$ which system is closely related to $SrFeO_3$ [15]. This also indicates that in $La_{0.8}Sr_{0.2}Fe_{0.3}Co_{0.7}O_3$, iron is located in Sr^{2+}-rich areas
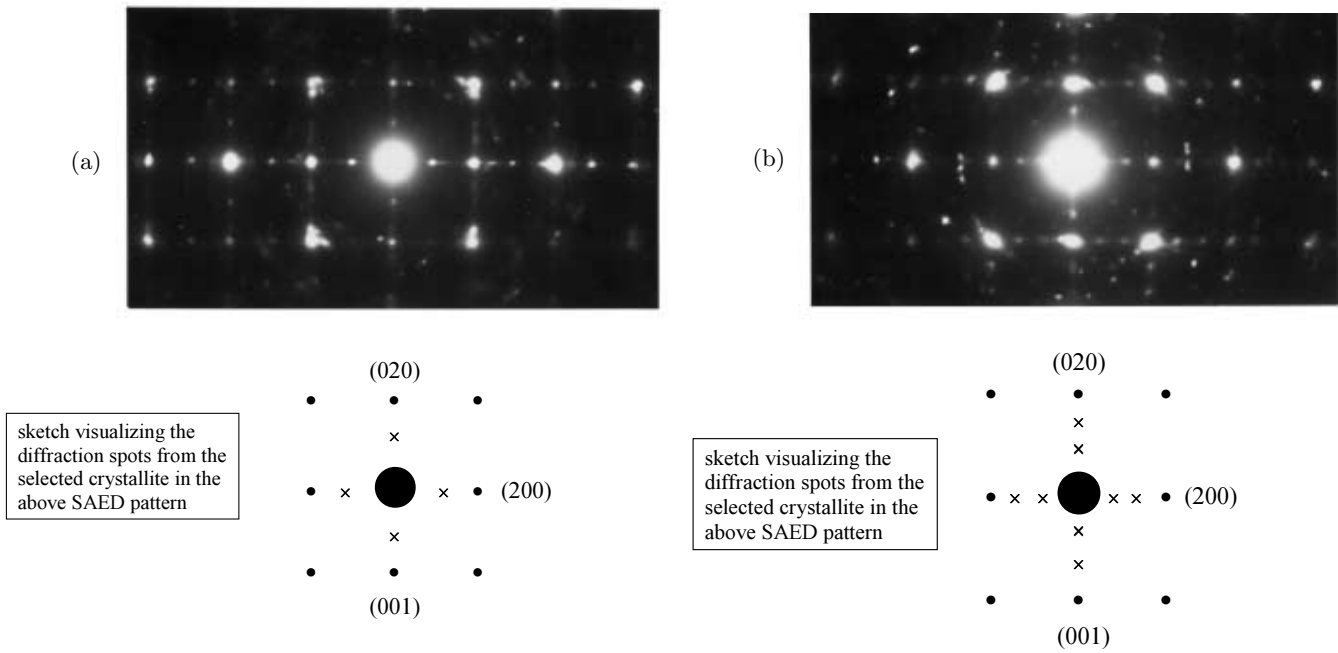
Fig. 6. Typical SAED patterns taken on the $La_{0.8}Sr_{0.2}Fe_{0.05}Co_{0.95}O_3$ sample from the $\langle 001 \rangle$ direction where the weak superreflection spots indicate lattice (a) doubling and (b) tripling. The sketches attached to the SAED patterns visualize which spots arise from the selected individual crystallite only.
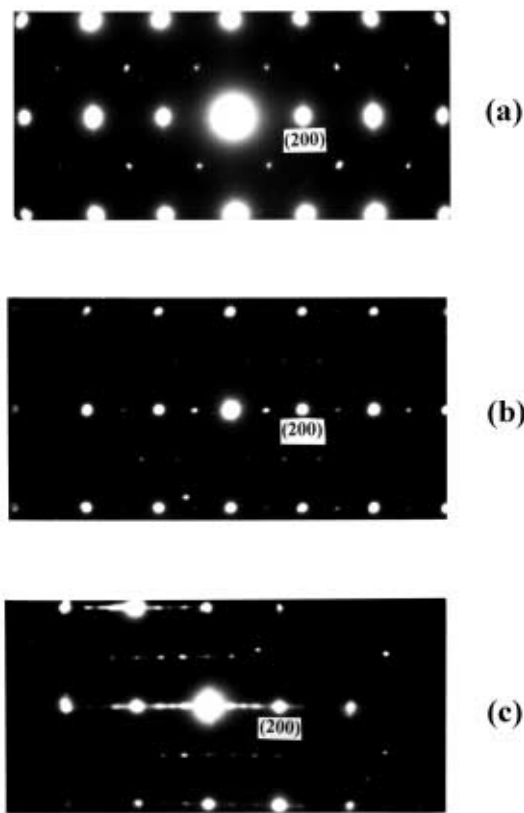

Fig. 7. Typical SAED patterns taken from the $\langle 021 \rangle$ direction, where the weak superreflection spots indicate the superstructures in samples (a) at the smallest Fe-content ($x = 0.025$) and at (b) $x = 0.15$ and (c) $x = 0.30$.
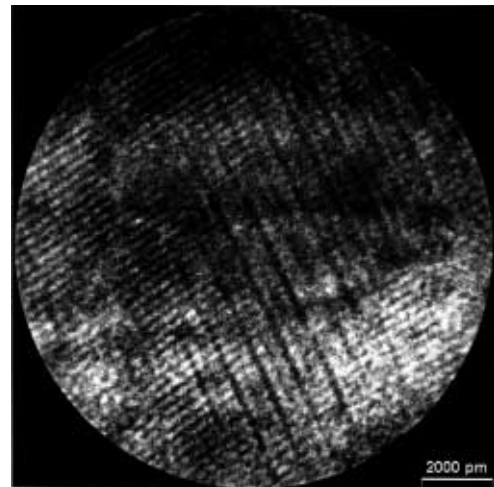
Fig. 8. The high-resolution TEM picture taken on the $La_{0.8}Sr_{0.2}Fe_{0.3}Co_{0.7}O_3$ sample shows an anisotropic ordered perovskite-type structure.

where the missing positive charge needs to be balanced by oxygen vacancies.

The broad absorption lines in the ^{57}Fe Mössbauer spectrum refer to the existence of a distribution in the quadrupole interaction probed by the ^{57}Fe nucleus. A distribution of this kind indicates the existence of several slightly different iron microenvironments in the sample. Such slight differences in the local microenvironment of iron may be caused by the different local distortions of
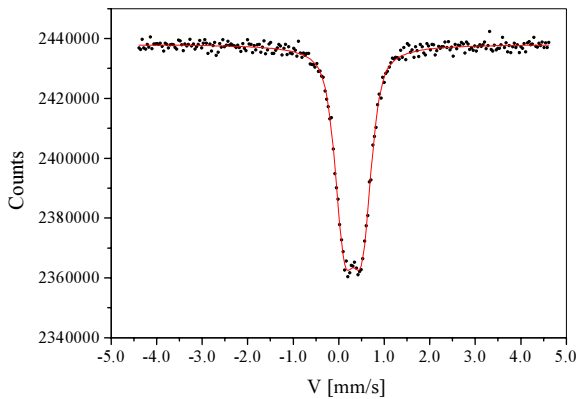
Fig. 9. ^{57}Fe Mössbauer spectrum of $La_{0.8}Sr_{0.2}Fe_{0.3}Co_{0.7}O_3$ taken at 290 K.

the lattice around the Fe^{3+} cations, presumably originating from the inhomogeneous cation substitution.

The domain structure observed for the $La_{0.8}Sr_{0.2}Fe_xCo_{1-x}O_3$ system ($x = 0.025, 0.05, 0.10, 0.15, 0.20, 0.3$) is similar to that already observed for the $La_{1-y}Sr_yCoO_3$ system in reference [16] where the formation of domains was explained as a consequence of the ordered lattice substitution of the La atoms by Sr atoms. In the present case, however, the ordered structures became more complicated, presumably as an effect of the partial Co/Fe substitution. In the presence of Fe, anisotropic lattice doubling or tripling takes place. Furthermore, in the sample with the largest Fe content where the ratio of Co/Fe is near to 3/1, in one direction fourfold lattice parameter was observed, too. The appearance of the fourfold lattice parameter can be explained by the ordered lattice substitution of Co by Fe in relatively large areas. The lattice doubling and tripling could be a result of the ordered substitution either of Co by Fe or La by Sr, accompanied by local concentration fluctuations.

From a comparison of the structural and MR properties of La-Sr-Co-O and La-Co-Mn-O films, it was concluded [17] that the existence of a domain structure reduces the MR ratio. It was established that, although each domain may exhibit a high MR ratio due to its anisotropic superstructure, the overall MR ratio of the entire material may not be high. This is because the small-sized, anisotropic domains are distributed along the three axes with equal probability, and the spatial average may reduce the MR ratio.

In contrast to the above conclusion, the present La-Sr-Fe-Co-O samples in which the size of the randomly distributed domains are similar exhibit large MR ratios, in spite of their complicated domain structure. This effect may find an explanation in the anisotropic nature of the domain structure of the Fe-containing samples.

5 Conclusions

A crystallographic study by XRD and TEM revealed that even the smallest investigated amount of Fe-doping causes remarkable changes in the crystal structure of the parent $La_{0.8}Sr_{0.2}CoO_3$ material, in correlation with the changes of their MR properties detected previously [1].

The atomic resolution TEM images, as well as the appearing superreflections in the corresponding SAED patterns, revealed a superstructure in the Fe-containing samples. The details of the superstructure were found to depend on the concentration of iron.

^{57}Fe Mössbauer spectroscopy indicated that in $La_{0.8}Sr_{0.2}Fe_{0.3}Co_{0.7}O_3$ the Fe^{3+} ions are located in Sr^{2+}-rich areas, coexisting with oxygen vacancies to balance the missing positive charge.

An ordered lattice substitution arising because of local composition fluctuations was found to take place between the La/Sr and the Co/Fe atoms, resulting in an ordered domain structure the existence of which can explains the large MR ratio of these La-Sr-Fe-Co-O compounds.

References

1. A. Barman, M. Ghosh, S. Biswas, S.K. De, Appl. Phys. Lett. **71**, 3150 (1997).
2. S. Yamaguchi, Y. Okimoto, Y. Tokura, Phys. Rev. B **55**, 8666 (1997).
3. A. Mineshige, M. Inaba, T. Yao, Z. Ogumi , K. Kikuchi, M. Kawase, J. Solid State Chem. **121**, 423 (1996).
4. J.B. Torrance, P. Lacorre, C. Asavaroengchai, R.M. Metzger, Physica C **189**, 351 (1991).
5. D.D. Sarma, A. Chainani, R. Cimino, P. Sen, C. Carbone, M. Mathew, W. Gudat, Europhys. Lett. **19** (1992) 351.
6. A. Chainani, M. Mathew, D.D. Sarma, Phys. Rev. B **46**, 9976 (1992).
7. V. Golovanov, L. Mihály, A.R. Moodenbaugh, Phys. Rev. B **53**, 8207 (1996).
8. G. Briceno, H. Chang, X. Sun, P.G. Schultz, X.-D. Xiang, Science **270**, 273 (1995).
9. R. Mahendiran, A.K. Raychaudhuri, A. Chainani, D.D. Sarma, J. Phys. Cond. Matt. **7**, L561 (1995).
10. J. Rodriguez-Carvajal, FullProf version 3.5 December 1997, ILL.
11. Z. Klencsár, E. Kuzmann, A. Vértes, J. Radioanal. Nucl. Chem. **210**, 105 (1996).
12. G.H. Jonker, J.H. van Santen, Physica **19**, 120 (1953).
13. R.D. Shannon, Acta Crystallogr. A **32**, 751 (1976).
14. N.N. Greenwood, T.C. Gibb, *Mössbauer Spectroscopy* (Chapman and Hall Ltd., London, 1971), 280 pp.
15. P.K. Gallagher, J.B. MacChesney, D.N.E. Buchanan, J. Chem. Phys. **45**, 2466 (1966).
16. Z.L. Wang, J. Zhang, Phys. Rev. B **54**, 1153 (1996).
17. S. Jin, M. McCormack, T.H. Tiefel, R. Ramesh, J. Appl. Phys. **76**, 6929 (1994).